Journal of Thermal Analysis and Calorimetry (2024) 149:10321–10333
https://doi.org/10.1007/s10973-024-13080-0

Staged thermal runaway behaviours of three typical lithium-ion batteries for hazard prevention

Yang Xiao[1,2] · Jia-Rong Zhao[1] · Lan Yin[1,2] · Bei Li[3] · Yuan Tian[4]

Received: 16 July 2023 / Accepted: 16 March 2024 / Published online: 16 April 2024

Abstract

Thermal runaway (TR) considerably restricts the applications of lithium-ion batteries (LIBs) and the development of renewable energy sources, thus causing safety issues and economic losses. In the current study, the staged TR characteristics of three LIBs are examined using a self-built experimental platform and cone calorimeter. The results indicate that the TR of the ternary lithium and lithium cobalt batteries successively underwent the following stages: smoke production, swelling, bursting and combustion. By contrast, the lithium iron phosphate battery experiences smoulder instead of combustion during TR process. The TR time of the ternary lithium, lithium cobalt oxide and lithium iron phosphate batteries are 728 s, 689 s and 849 s, and the critical temperatures are 260.02 °C, 240.84 °C and 290.88 °C, respectively. Moreover, the lithium cobalt oxide battery has the largest heat release of 0.027 MJ m^{-2}, the ternary lithium battery presents the most mass loss rate of 0.75 g s^{-1}, and the lithium iron phosphate battery produced the largest smoke, CO and CO_2 during the TR process. These results reveal the safety and stability of three LIBs and can be beneficial for studies on the proactive process safety and potential hazard prevention of LIBs.

Keywords Renewable energy · Cathode material · External heating condition · Peak TR temperature · Critical temperature

Introduction

Rapid consumption of non-renewable resources and massive emission of carbon dioxide since the Industrial Revolution in the nineteenth century have substantially increased the damage caused to the environment [1]. To reduce this damage, renewable energy development, transformation and storage technology have improved considerably. LIBs have been increasingly used because of their various advantages, including high energy density, high power energy, favourable cycle performance, long life cycle and environmental friendliness [2]. However, with an increase in the capacity and specific capacity of LIBs, the TR of LIBs has caused numerous fires and explosion incidents involving energy storage power stations, computers, mobile phones and electric cars (Fig. 1a), including LIB energy storage system accidents in South Korea [3], the Tesla electric car battery fire [4] and Samsung Galaxy Note 7 mobile phone explosions [5]. Therefore, concerns have been raised regarding the use of LIBs in terms of personal safety, commercial promotion, social benefits and the ecological environment. The TR characteristics of LIBs are widely studied in the renewable energy industry.

TR is the primary cause of accidents involving LIBs [5–9]. TR refers to the process in which uncontrollable exothermic chemical reactions occur inside the battery under severe conditions (heating, overcharging, short circuit, puncture, extrusion, etc.) [10–14], resulting in an increase in internal temperature, pressure, organic electrolyte production and decomposition products (Fig. 1b). Combustion or explosion accidents occur when the pressure and

✉ Yang Xiao
xiaoy@xust.edu.cn

1 School of Safety Science and Engineering, Xi'an University of Science and Technology, No. 58, Yanta Mid. Rd., Xi'an 710054, Shaanxi, People's Republic of China

2 Shaanxi Key Laboratory of Prevention and Control of Coal Fire, Xi'an University of Science and Technology, Xi'an 710054, Shaanxi, People's Republic of China

3 School of Chemical Engineering, Dalian University of Technology, Dalian 116024, Liaoning, People's Republic of China

4 Institute of Energy and Sustainable Development, School of Engineering and Sustainable Development, De Montfort University, Leicester LE1 9BH, UK

temperature of LIBs reach the upper limit. The methods, such as differential scanning calorimeter (DSC), accelerating rate calorimeter (ARC), C80 micro-calorimeter, VSP2 adiabatic calorimeter, oven box and numerical simulation methods commonly used to determine the TR of LIBs [15–21].

The TR of LIBs can be divided into different stages and exhibit different behaviours. Wang et al. [4] characterised the TR of fully charged 50 Ah $LiNi_xCo_yMn_{1-x-y}O_2$/graphite batteries by using different heating methods and divided the TR into four steps, namely smouldering without flame, gas release or explosion, flame and reignition stages. Ping et al. [22] divided the combustion behaviours of a 50 Ah lithium-iron phosphate/graphite battery pack into six stages, including expansion, jet flame, stable combustion, a second cycle of a jet flame followed by stable combustion, abatement and extinguishment. TR would increase the risk of a fire accident by triggering combustion and resulting in heat release [23, 24], releasing toxic and harmful gases [25, 26] and generating a large amount of smoke. The combustible material ejected from LIBs, high-temperature electrode active substance and oxygen are the three main conditions required for LIBs combustion [27]. CONE is widely used to investigate the combustion characteristics of LIBs. Fu et al. [28] used CONE to examine the effect of the stage of charge (SOC) on the burning behaviours of 18,650 LIBs. Zhong et al. [29] used an improved CONE to examine the combustion behaviours of 18,650 LIBs and measured the changes in the law of temperature, the heat release rate (HRR) and gaseous products. Yang et al. [30] developed a concentration device to analyse CO and CO_2 gases released during the TR of LIBs. The experimental results indicated that ambient temperature, battery capacity and heating power were proportional to the gas concentration.

Numerous factors affect the thermal behaviours and safety of LIBs. The electrochemical behaviours of LIBs were directly proportional to the SOC [31]. LIBs with a higher capacity tended to have higher TRs [20]. Moreover, different heating regions and heating power are crucial for the TR of LIBs [21]. The cathode material released the maximum amount of heat during the TR of the battery, considerably reducing the safety of LIBs [32]. Therefore, research on different cathode materials used in LIBs can help improve the safety of LIBs.

In this study, we investigated the stability of cathode materials used in three typical LIBs. $LiCoO_2$ is the first commercial cathode material used in LIBs. Despite its demerits, including high cost and the ability to cause severe pollution, $LiCoO_2$ has been widely used in recent years. Currently, the Tesla Roadster are powered by $LiCoO_2$ batteries [33]. Lithium iron phosphate batteries have higher stability due to their olivine structure. Moreover, these batteries are safe to use and environmentally friendly, exhibit superior cycling performance, require low-cost raw material and have a high TR critical temperature and low self-discharge rate [34]. In addition, ternary lithium batteries, which integrate the advantages of $LiCoO_2$, $LiMnO_2$ and $LiFePO_4$, demonstrate high energy density and favourable overall performance. Ternary lithium batteries have been widely used in notebooks, new energy vehicles and energy storage systems in recent years [35].

To sum up, many studies have found that battery capacity, heating mode, SOC and other factors have a significant influence on the TR process and combustion characteristics of LIBs, and pointed out that the cathode material of the battery is the key to high safety of LIB. However, the current research focuses on the TR of the 18,650-type LIBs, single LIBs and related materials, there are few comparative studies on TR of soft-package LIBs with different cathode materials, and the experimental methods used are relatively simple. Based on it, we evaluated the TR and combustion

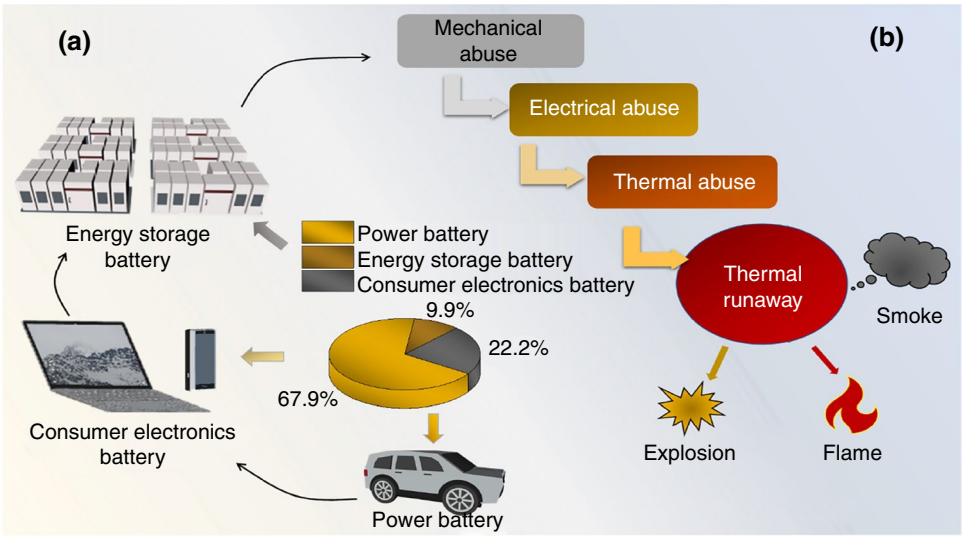

Fig. 1 Distribution of LIBs in different sectors in 2021 of China (**a**) and the reasons for LIBs TR (**b**)

characteristics of soft-package LIBs containing three cathode materials by using an independently built experimental platform and CONE in this work. Furthermore, we combined data analysis with images to compare variations in parameters in the various stages of three typical types of LIBs to comprehensively analyse the TR behaviours of LIBs. Subsequently, some combustion characteristic parameters of LIBs were explored, which may provide a reference for the implementation of strategies for process safety and potential hazard prevention of LIBs.

Materials and methods

The battery

Three typical soft-package LIBs with different cathode materials including $LiN_{1/3}Mn_{1/3}Co_{1/3}O_2$, $LiCoO_2$ and $LiFePO_4$ were selected, namely ternary lithium battery, lithium cobalt oxide battery and lithium iron phosphate battery, respectively. Figure 2 presents the structure of the soft-package LIBs and the working principle. As Fig. 2c shows, $LiN_{1/3}Mn_{1/3}Co_{1/3}O_2$ and $LiCoO_2$ have the same crystal structure as a-$NaFeO_2$ and the crystal structure of $LiFePO_4$ is olivine-type [36, 37]. The anode materials of the three LIBs are all carbon, and the electrolyte mainly consists $LiPF_6$ and solvents ($C_3H_4O_3$, $C_4H_6O_3$). The nominal voltage of three LIBs are 3.7 V, 3.2 V, and 4.2 V. Otherwise, the capacity values of the three LIBs were all the same as 2 Ah. Before testing, we first discharged the new battery and then charged those to 100% SOC at the same constant current.

Apparatus and procedures

As Fig. 3 presents, this work carried out a self-built experimental platform and CONE to explore the TR behaviours of three typical LIBs. The structure and principle of the apparatus are as follows.

Self-built experimental platform

Figure 4 presents the schematic of the self-built experimental platform. The platform consists of an infrared thermal imager (- 20 °C to 750 °C), a copper heating plate (150 ×

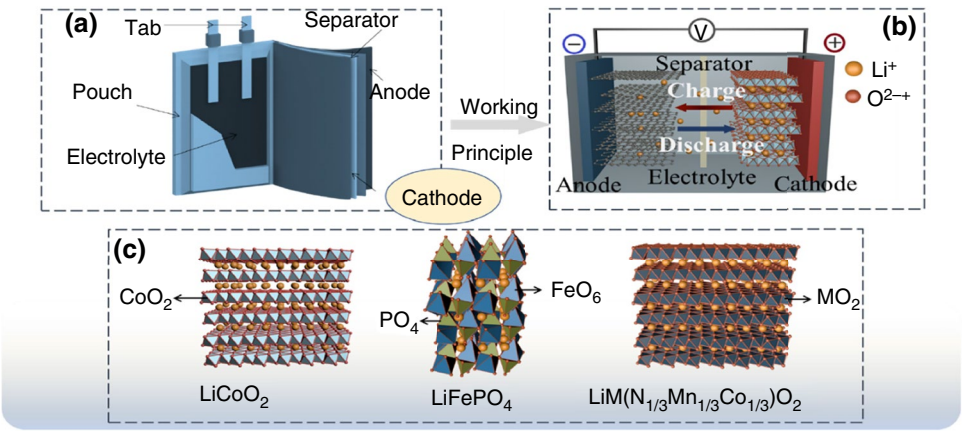

Fig. 2 Structure (**a**) and working principle (**b**) of the soft-package LIBs (**a**) and the crystal structure of three cathode materials (**c**)

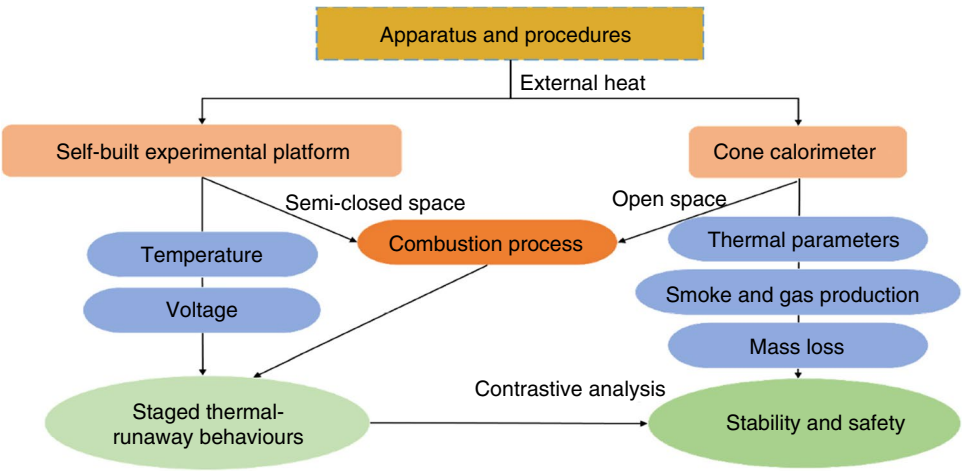

Fig. 3 Technology roadmap for the experiments

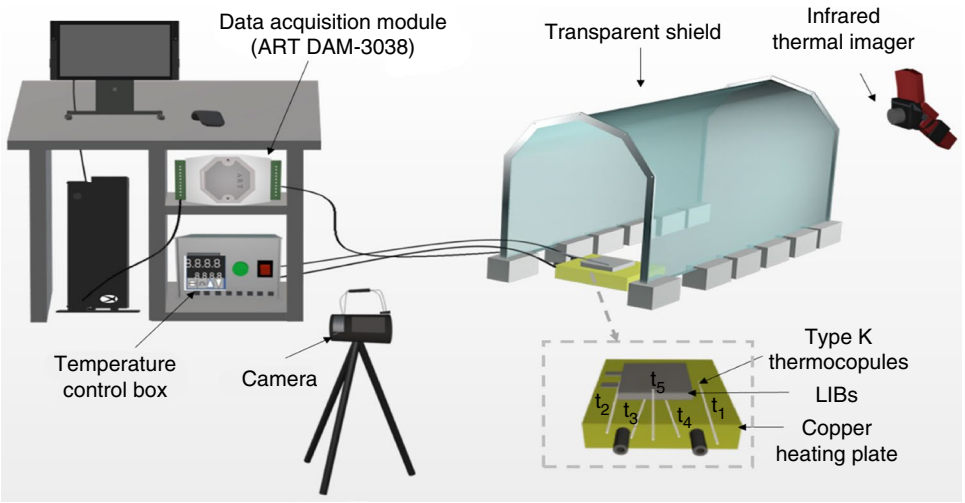

Fig. 4 Schematic of the self-built experimental platform

150 × 150 mm; 0–550 °C), a temperature control box (180 × 130 × 110 mm; 0–600 °C), a digital video camera (Sony, HDR-CX405, 1080 p), and a data acquisition and storage system (0–1000 °C) composed of thermocouples, a data acquisition module (ART DAM-3038), wires and a computer. We did preliminary experiments to detect the accuracy of the self-built experimental platform before tests.

As presented in Fig. 4, the LIBs were heated using a copper heating plate and an intelligent temperature controller. An infrared thermal imager was placed 2 m to the front left of the LIBs to capture the thermal image of the change in the temperature of the LIBs in real time. Furthermore, a camera placed 2 m to the front right of the LIBs was used to record the combustion process during TR. The positive and negative terminals of the LIBs were connected by wires to monitor voltage. Five *K*-type WRNK-191 thermocouples were arranged to monitor the change in the temperature of the battery in real time, including the temperature of the heating plate (t_1), the temperature near the LIB electrode lug (t_2), the temperature of the LIB hot surface (t_3, t_4) and the temperature of the LIB cold surface (t_5). In addition, to further investigate the TR characteristics of LIBs, the critical temperature values of the LIBs were examined by altering heating methods. The critical temperature was defined as the temperature value at TR occurred. Set initial temperature at 150 °C, and increase the temperature by 10 °C unless the LIBs lost thermal control. Then, each temperature gradient was maintained for 5–8 min until the occurrence of the TR of the LIBs. At this moment, the values of the temperature control box set were the critical temperature of LIBs.

Cone calorimeter

The combustion characteristics of the three LIBs were investigated using CONE. The HRR, total release rate (THR), smoke produce rate (SPR), gas generation and mass loss were measured. The three LIBs were placed in a sample cell individually during the experimental tests. We covered the sample by using a wire grid to prevent the generation of explosion sparks that damage the cone heater. The sample was heated by the cone heater, and combustion gaseous products were collected using an exhaust hood and transported using a ventilation system. The N_2, CO and CO_2, O_2, mass, soot flow and baseline calibrations of CONE were performed before the experiments. A gas analyser was employed to measure the production of O_2, CO and CO_2. The experimental temperature was increased from ambient temperature to 400 °C. When the flame was completely put out, the test was terminated.

Results and discussion

Thermal runaway of three LIBs

Thermal runaway behaviours

As Fig. 5 shows, different LIBs performed various behaviours and experienced three steps from start to finish during the heating by a self-built experimental platform. Firstly, all the LIBs were observed to produce smoke and gases with a pungent odour near the electrode lug at different points of time, including CO, HF, H_2, CO_2, SO_2, CH_4, C_2H_4, HCl and other toxic gases [31, 32]. Moreover, the shell combustion of the battery produced gases with a pungent odour. The smoke volume increased with the temperature rise of the heating plate. Then, the three LIBs began to swell after the production of smoke and swelled to its limit after a short time. Subsequently, the ternary lithium battery and lithium cobalt oxide battery ejected numerous dazzling sparks near the electrode lug after swelling and bursting, indicating the occurrence of a TR. After approximately 7–8 s, the two LIBs

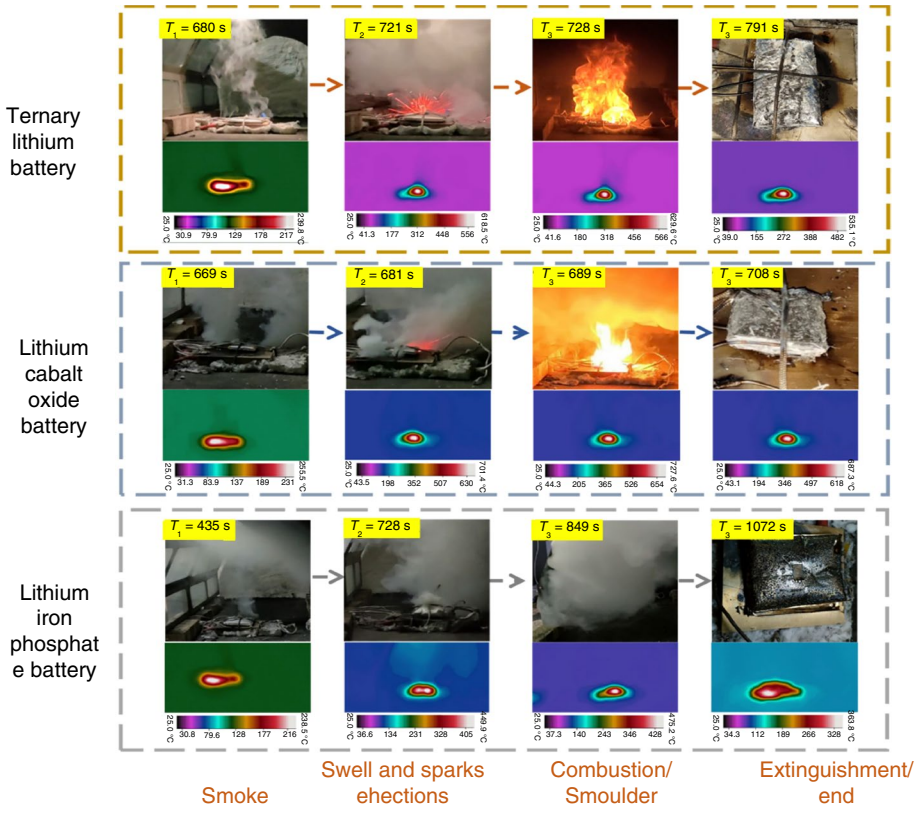

Fig. 5 Behaviours of the three batteries using the self-built experimental platform

reached a stable combustion stage and burned silently. The rapid swelling and combustion of the LIBs were primarily due to the swift exothermic reaction occurring between the electrolyte and cathode material, resulting in the generation of a large amount of combustible gas (CH compound) and combustion-supporting gas (O_2) as Eqs. (1–3) [38]. However, the TR behaviours of the lithium iron phosphate battery showed large differences under external heating as shown by the literature [39]. The battery ejected a large amount of electrolyte after it was swollen to its limit at 817 s, and then, smouldering occurred with the marked production of abundant smoke. After approximately 30 s, the laboratory was filled with smoke, and the battery did not stop reacting until 1076 s. Further observation revealed that the surface morphology of the LIBs was significantly different after TR. The ternary lithium and lithium cobalt oxide batteries completely burned and formed multilayer grey substances. However, the lithium iron phosphate battery reacted incompletely, and some dense black electrolyte was attached to the battery surface. This is because the strong covalent P–O bonds in the cathode inhibit the production of oxygen [40], and release much less oxygen during the cathode decomposition compared with other LIBs causing the combustion of the electrolyte significantly inhibited [41]. The absence of oxygen causes smouldering rather than steady combustion. Additionally, by observing the changes in the infrared image depicted in Fig. 5, it can be observed that as the temperature increases, there is a sharp rise in the overall temperature of the three LIBs during the second stage. The temperature distribution exhibits a gradual decrease from inner to outer regions, indicating that TR of the LIBs initiate from a specific area rather than undergoing simultaneous reaction.

$$\mathrm{Li_xCoO_2} \rightarrow x\mathrm{LiCoO_2} + 1/3(1-x)\mathrm{Co_3O_4} + 1/3(1-x)\mathrm{O_2}\uparrow \quad (1)$$

$$\mathrm{NCM(R3-M)} \rightarrow \mathrm{(Mn,Ni)(Fm3m)} + \mathrm{CoO} + \mathrm{O_2}\uparrow \quad (2)$$

$$2\mathrm{FePO_4} \rightarrow \mathrm{Fe_2P_2O_7} + 0.5\mathrm{O_2}\uparrow \quad (3)$$

In summary, the TR process of the ternary lithium battery and lithium cobalt oxide battery differed from that of the lithium iron phosphate battery. A mass of previous works in the literature has shown that lithium iron phosphate battery is the safest among many other LIBs chemistries [42, 43]. The time required from the production of smoke to the end of the reaction for the ternary lithium battery and lithium cobalt oxide battery was approximately 60 s shorter than what was required for the lithium iron phosphate battery. In addition, the combustion of the ternary lithium battery and lithium cobalt oxide battery were observed, and the smoke produced by these two LIBs was less than that produced by the lithium iron phosphate battery. Although the combustion phenomenon was not observed after the bursting of

the lithium iron phosphate battery, the generation of smoke and gases with a pungent odour was noted. The lithium iron phosphate battery might explode if the generated combustible gas reaches the explosion limit and encounters external ignition sources as reported in Ref. [44].

However, as Fig. 6 illustrates, the behaviours of the three LIBs have shown different under the CONE test. With the constant increase in radiation flow, the lithium iron phosphate battery burned and produced less smoke unlike the results reported above. This finding was ascribed to the fact that the self-built platform set up in the laboratory required placing the battery in a semi-closed space leading to the accumulation of substances generated around the battery and less oxygen released during the decomposition of the lithium iron phosphate battery. Due to these two factors, insufficient oxygen was provided into the interior of the battery. However, a CONE was used in this experiment, smoke produced by the combustion of the battery was discharged through the exhaust pipe and the pen space of LIBs placed provided adequate oxygen from outside. Figure 6 also points out the time to occur combustion of the three LIBs are 535, 477 and 555 s, respectively. The lithium cobalt oxide battery occurred TR at the shortest reaction time, whereas the lithium iron phosphate battery required the longest time. Such a finding indicated that the lithium iron phosphate battery possessed the highest thermostability.

Variation of temperature and voltage

Figure 7 depicts changes in the temperature of the three LIBs. Five stages were divided by temperature change curves, and their TR behaviours were analysed. In stage I, except for the cold surface, the temperature increased slowly and exhibited the same trend as the heating rate of the heating plate. This was because heat was mainly generated from the heating plate, whereas less heat was generated within the battery. Thermocouples arranged on the cold surface and electrode lug were far away from the heating plate, resulting in lower temperatures. In stage II, heat released by the chemical reactions of some active materials at high temperatures caused a slow increase in the heating rate. In stage III, the battery was swollen and exploded with a marked increase in temperature within a short time interval, reaching the highest heating rate. In stage IV, the temperature first increased and then decreased during the steady combustion period. The temperature reached the maximum while the heating rate decreased promptly. In stage V, a complete electrochemical reaction occurred, and the temperature decreased slowly after flame extinguishment.

As presented in Fig. 7a, the temperature of the LIB increased uniformly with the lifting of the heating plate at the initial heating stage. At 723 s, the battery temperature increased sharply, reaching the maximum value of 637.23 °C within 8 s, and the maximum temperature reached 63.89 °C s^{-1} after 20 s. Figure 7b depicts that the TR of the lithium cobalt oxide battery occurred at 684 s while the temperature reached the maximum value of 859.53 °C and the temperature increased to 143.64 °C s^{-1} after 20 s. Figure 7c indicates that the lithium iron phosphate battery was out of control at 852 s. Meanwhile, the maximum temperature of the battery reached 488.54 °C, and the temperature increased rapidly by 29.01 °C s^{-1} after the explosion of the battery. Under the same heating conditions, the lithium cobalt oxide battery reached TR earlier and attained higher temperature and heating rate values than the lithium ternary battery and the lithium iron phosphate battery.

The voltage of the ternary lithium battery and lithium cobalt oxide battery fluctuated after the swelling of the battery (Fig. 7d). The voltage dropped to 0 V within 8–10 s after the occurrence of TR. The voltage exhibited no prominent change before the TR occurred; thus, the voltage cannot indicate the occurrence of TR. However, the voltage of the lithium iron phosphate battery was not decreased to 0 V immediately. The voltage exhibited apparent fluctuations in stage IV after the material inside the battery decomposed incompletely.

Critical temperature of thermal runaway

To determine the TR characteristics of the LIBs, the temperature was set at 150.00 °C first and then increased by 10 °C every 5–8 min until the occurrence of the TR of the

(a) 535 s **(b)** 465 s **(c)** 555 s

Fig. 6 Combustion stage of three LIBs [ternary lithium battery (**a**), lithium cobalt oxide battery (**b**) and lithium iron phosphate battery (**c**)] using a CONE

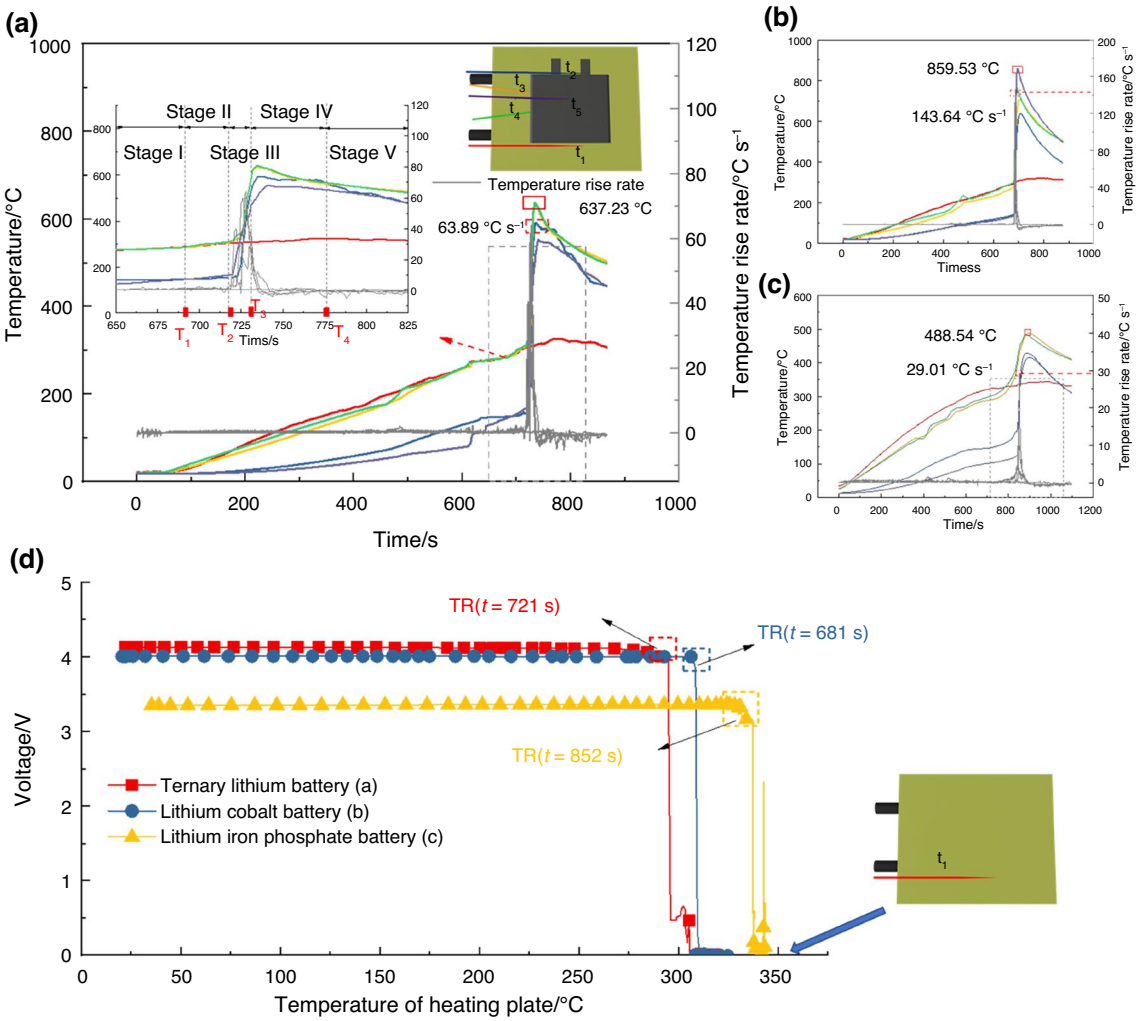

Fig. 7 Temperature and temperature increase rate curves of five faces and division of TR stages for the ternary lithium battery (**a**), lithium cobalt oxide battery (**b**), lithium iron phosphate battery (**c**) and the voltage of three typical LIBs (**d**)

LIBs. Changes in the TR critical temperature, voltage and the behaviours of the three LIBs were determined (Fig. 8). We observed that if the temperature of the heating plate remained unchanged after the production of smoke and the slight swelling of the battery, the TR phenomenon did not occur immediately. As the temperature of the heating plate increases, the battery became swollen to its limit. When the temperature of the heating plate remained unchanged, TR easily occurred in a short period. Unlike the ternary lithium battery, the lithium cobalt oxide and lithium iron phosphate batteries exhibited slight air leakage at 220.00 and 160.00 °C, respectively, with a concurrent decline in voltage during the test. With an increase in the heating plate temperature, the voltage of the lithium iron phosphate battery increased again until it decreased to 0 V after TR. The critical temperatures for TR of the three LIBs were 260.02, 240.84 and 290.88 °C, respectively, which indicated that lithium iron phosphate battery had the highest thermal stability than others.

Combustion characteristics of three LIBs

Thermal parameters

HRR and THR are crucial elements governing thermal hazards, they must be considered while investigating the fire or explosion risks of the LIBs. Figure 9 depicts the HRR and THR variation curves of the three LIBs under the constant radiation current. The three LIBs had no perceivable heat release until the battery began to burn. During the combustion stage, the HRR of ternary lithium battery, lithium cobalt oxide battery and lithium iron phosphate battery are rapidly increased and reached the maximum at 428.78, 508.87 and 254.93 kW m^{-2}, respectively, and then decreased at once.

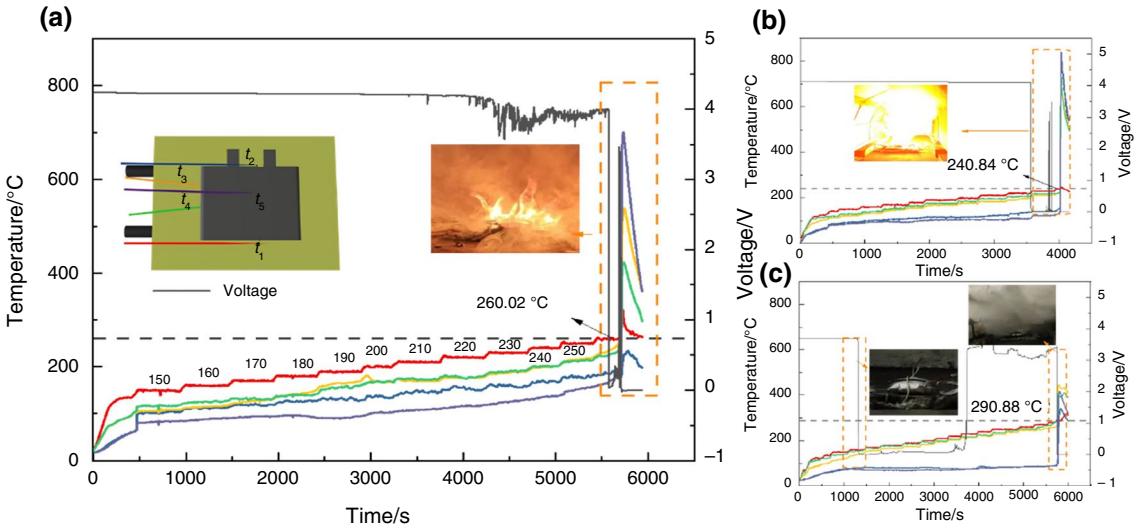

Fig. 8 Temperature and voltage versus time curves of the ternary lithium battery (**a**), lithium cobalt oxide battery (**b**) and lithium iron phosphate battery (**c**)

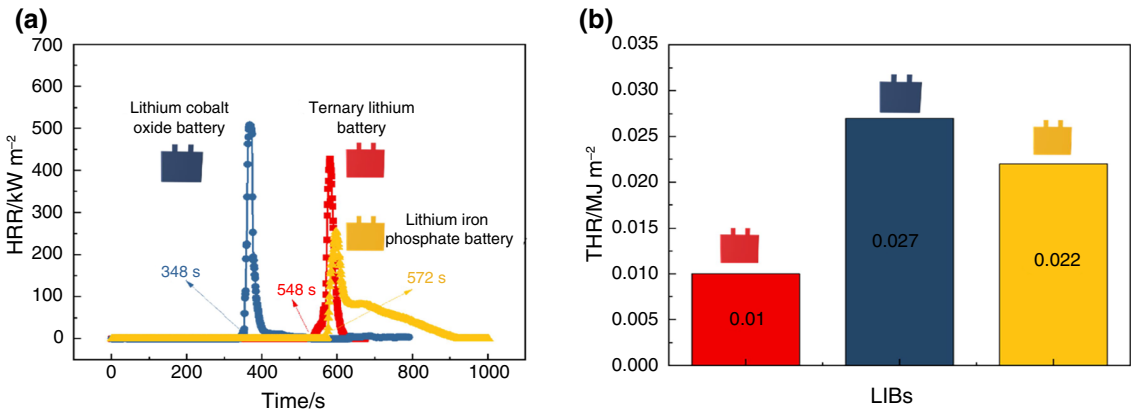

Fig. 9 HRR (**a**) and THR (**b**) curves of three LIBs

The lithium cobalt oxide battery released heat first, followed by the lithium iron phosphate battery. As Fig. 9a shows, the HRR of the lithium cobalt oxide battery rapidly increased at first, whereas that of the lithium iron phosphate battery was more stable than those under the same heating conditions. In addition, the THR of the lithium cobalt oxide battery were the highest reaching 0.027 MJ m^{-2}, indicating that the lithium cobalt oxide battery had a higher risk of TR than the other two LIBs.

Smoke and gas production

Abundant CO, CO_2, H_2, CH_4, C_2H_2, C_2H_4, PF_5, and other poisonous and harmful gases can be generated during the overheating of the LIBs [32], resulting in hypoxia, asphyxia, poisoning and other conditions in the human body. A CONE can be utilised to quantitatively analyse smoke and gases produced during the TR of the LIBs. The smoke produce rate (SPR) and total smoke production (TSP) of the three LIBs are presented in Fig. 10. The SPR of the three LIBs was low before combustion, but rapidly increased when they were out of control, reaching the maximum values of 0.13, 0.08 and 0.21 m^2 s^{-1}, respectively. The largest TSP of the lithium iron phosphate battery was 6.8 m^2.

Figure 10c, d presents the concentration variation of CO and CO_2. Both them were generated at the beginning of the smoking stage of the LIB. As temperature rises, the concentrations of CO and CO_2 increased markedly until the end of combustion. The concentration of CO_2 is significantly higher than CO. The generation of CO_2 was related to certain chemical reactions, including the decomposition

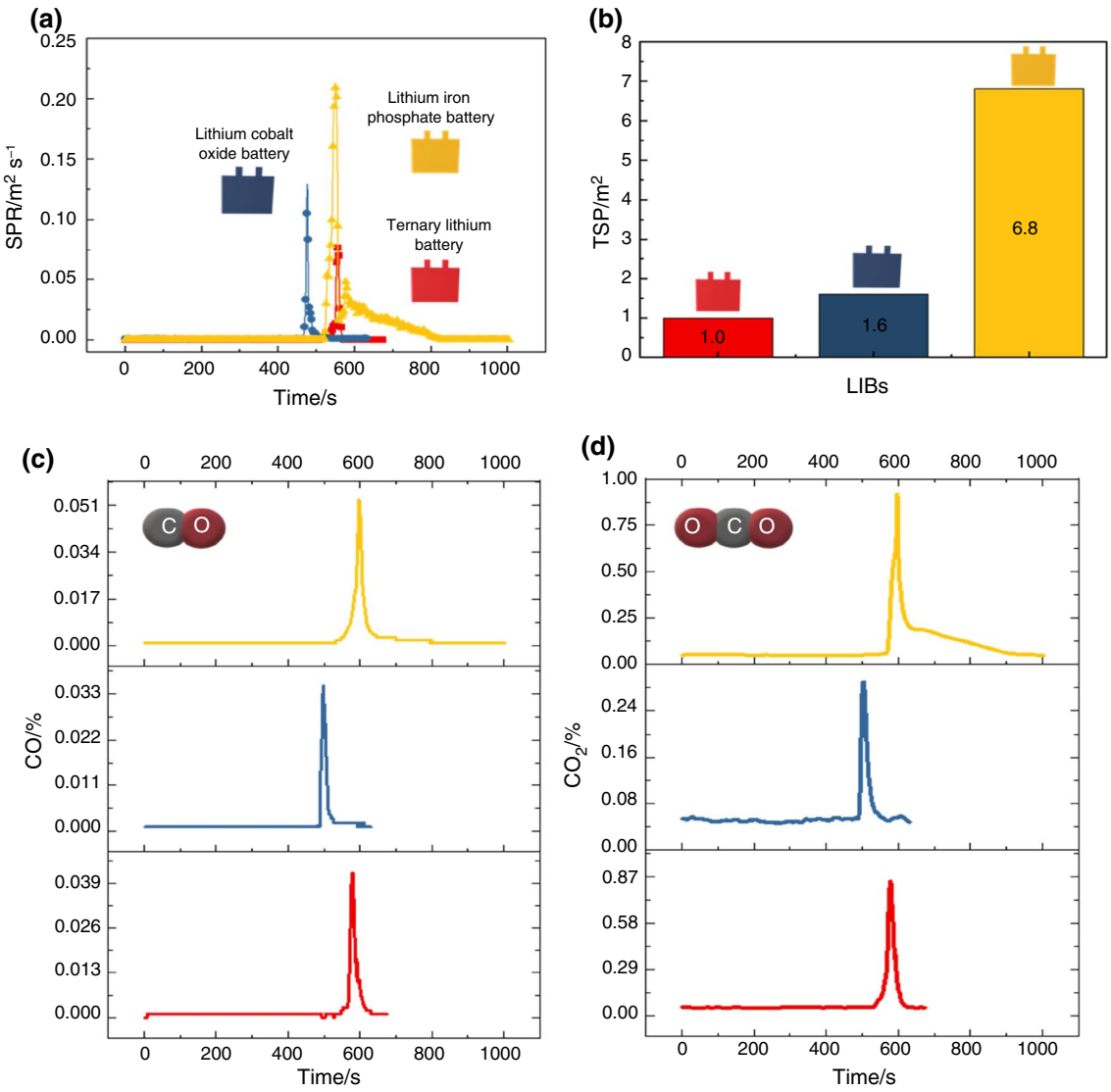

Fig. 10 Smoke parameters of three LIBs: SPR (**a**), TSR (**b**), content variation in CO (**c**) and CO_2 (**d**) produced by three LIBs

of the solid electrolyte interface film (Eqs. 4, 5) and the reaction between the electrolyte and cathode material as Eqs. (6) and (7) shows [38]. Some CO was formed by the reaction of the cathode electrode of the battery with the resulting CO_2 (Eq. 8), and it can also be produced from incomplete reactions (Eqs. 9 and 10) [4]. Therefore, the electrolyte of the LIBs and the anode material of the diaphragm exerted a substantial effect on the production of CO and CO_2. The toxic and harmful gaseous products indirectly reflected the risk of the TR of LIBs. The more the CO and CO_2 were produced, the higher the risk for the TR of the LIBs was.

$$(CH_2OCO_2Li)_2 \rightarrow Li_2CO_3 + C_2H_4 \uparrow + CO_2 \uparrow + 0.5O_2 \uparrow \quad (4)$$

$$Li_2CO_3 \rightarrow Li_2O + CO_2 \uparrow \quad (5)$$

$$2.5O_2 + C_3H_4O_3(EC) \rightarrow 3CO_2 \uparrow + 2H_2O \uparrow \quad (6)$$

$$4O_2 + C_4H_6O_3(PC) \rightarrow 4CO_2 \uparrow + 3H_2O \uparrow \quad (7)$$

$$2CO_2 + Li^+ + 2e^- \rightarrow CO \uparrow + Li_2CO_3 \quad (8)$$

$$O_2 + C_3H_4O_3(EC) \rightarrow 3CO \uparrow + 2H_2O \uparrow \quad (9)$$

$$2O_2 + C_4H_6O_3(PC) \rightarrow 4CO \uparrow + 3H_2O \uparrow \quad (10)$$

Mass loss

The mass variation of the three LIBs during TR can be divided into four stages as follows (Table 1). Stage I (t_{0-s})

Table 1 Some parameters for mass loss of the three LIBs by the CONE

LIBs	t_s/s	t_c/s	t_e/s	Δm_{s-c}/g	Δm_{c-e}/g	Δm_{0-t}/g	r_{max}/g s^{-1}
Ternary lithium battery	513	535	575	0.8	5.4	6.2	0.75
Lithium cobalt oxide battery	304	465	493	2.1	3.2	5.3	0.5
Lithium iron phosphate battery	406	555	887	4.3	4.1	8.4	0.4

is the heating stage of the battery from the beginning of the experiment to the beginning of the loss in mass, where the mass of the LIBs did not change markedly, principally because the LIBs were well sealed with no leaks or openings. The temperature did not reach the critical value for the reaction of the various components of the LIBs. The second stage was between the mass loss and combustion of LIBs (t_{s-c}), and high temperatures promoted chemical reactions within the battery, increased the gas production rate and caused the loss of mass of the battery at a relatively mild rate. Furthermore, the LIBs entered the TR period with a sharp decline in battery loss after combustion (t_{c-e}). During this period, the LIBs cathode material decomposes and releases a lot of heat, and the electrolyte burns, which are the direct causes of sharp mass loss; the mass loss of three LIBs reached 5.4, 3.2 and 4.1 g, respectively. The maximum battery mass loss rates (r_{max}, MLR) of the ternary lithium battery, lithium cobalt oxide battery and lithium iron phosphate battery were 0.75, 0.50 and 0.40 g s^{-1}, respectively. In stage IV, the mass loss had very little decrease, which indicated that combustion slowed down and terminated gradually. The total mass loss (Δm_{0-t}) was 6.2, 5.3 and 8.4 g, respectively. Although the ternary lithium battery exhibited the earliest mass loss, due to the presence of oxygen atoms, the degree of complete combustion during TR was higher than that of the other two types.

Discussion

In this work, two experiments were carried out to explore the TR behaviours, heat variation and mass loss of three LIBs from macroscopic. In fact, the TR process of LIB is so complicated mainly because of the complex thermochemical reactions inside the LIB during heating. The TR process of the LIB was further discussed by combining the experimental results with the previous references.

According to Fig. 11a, the TR process of LIBs can be summarised as four exothermic reactions between different materials, including the heating decomposition of the SEI layer, the reaction of anode material and electrolyte, the reaction of cathode material and electrolyte and electrolyte decomposition. Firstly, the metastable components of the SEI layer $(CH_2OCH_2Li)_2$ decompose exothermically at 90–120 °C [45]. As the temperature increases and the heat released from the decomposition of SEI layers increases, the organic solvents in the electrolyte react with the negative lithium releasing flammable hydrocarbon gases [46]. The gas generated not only increases smoke but also increases the internal pressure of the battery causing the slowly swelling of LIBs. Further increasing the temperature, the diaphragm of LIBs melts and causes a short circuit, triggering the continuous heat release of the battery [10]. The cathode material is partially decomposed to completely decomposed as the temperature increases, and then, the generated oxygen reacts with the electrolyte, releasing large heat

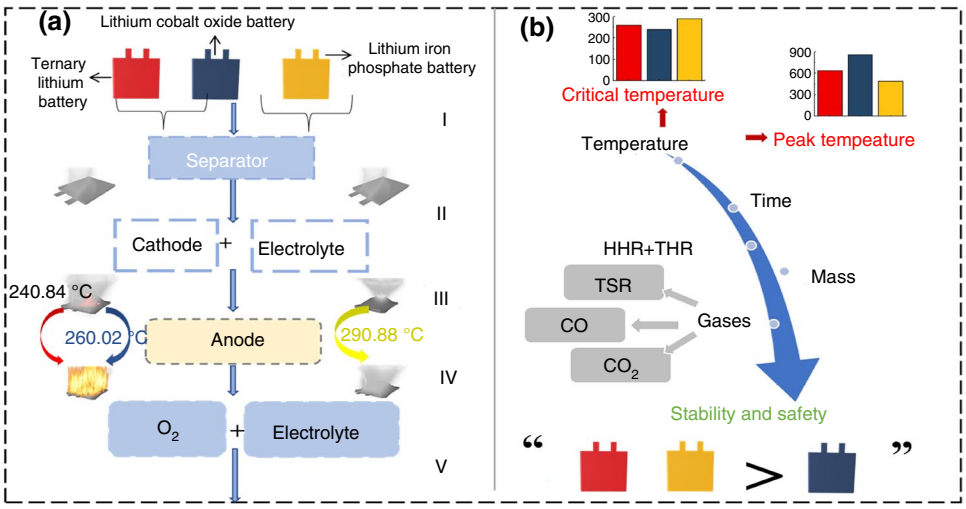

Fig. 11 TR behaviours with reaction process of LIBs

and producing a mass of combustible gases [46]. It can be known the decomposition temperature performs $LiCoO_2$ < $LiN_{1/3}Mn_{1/3}Co_{1/3}O_2$ < $LiFePO_4$ from the TR critical temperature of three LIBs in section "Critical temperature of thermal runaway." The large increase of heat and pressure inside the cell leads the LIB to swell and burst when it reaches the limit, ejecting a large amount of electrolyte. The electrolyte decomposed under high temperature, and the ternary lithium battery and lithium cobalt oxide battery enter a stable combustion stage with the assist of enough oxygen and combustible gas. But no combustion reaction occurs in lithium iron phosphate battery due to the lack of oxygen. The flammable gas, oxygen and heat released during the whole process are an indispensable part of TR, and the quality of the LIB is greatly reduced due to the decomposition and combustion of internal materials.

As Fig. 11b shows, the comprehensive analysis of temperature, reaction time, thermal parameters and gases of LIBs TR indicated that the lithium cobalt oxide battery has the lowest temperature condition required for TR, the highest heating rate during TR and the most heat release, followed by the ternary lithium battery. However, lithium iron phosphate batteries release the highest amount of smoke, CO and CO_2 after the TR, causing a higher risk of poisoning and suffocation. It indicates the stability and safety of the lithium cobalt oxide battery are the worst. Significantly, the lithium iron phosphate battery has higher thermostability but greater thermal runaway hazardness than the ternary battery.

These results shed light on the thermal runaway behaviours of three LIBs and the harm it can cause, propose some detection parameters for the TR of the LIBs, and provide a basis for the selection of lithium battery under different requirements. Combined with these results, it is recommended to avoid the use of lithium cobalt oxide batteries in daily needs or commercial applications. Besides, when analysing the risk of TR and fire in different LIBs, parameters such as temperature, heat, gas and time need to be comprehensively discussed. Significantly, it is necessary to prevent thermal runaway before it occurs for the time of thermal runaway of lithium batteries is too short. It is effective to analyse cathode materials, temperature and storage environment.

Conclusions

In this work, a new methodology is proposed to investigate the staged TR characteristics of the three LIBs comprehensively and clearly with different cathode materials through the combination of quantitative and qualitative, data analysis and image form by using a self-built experimental platform and CONE. The following primary conclusions were drawn:

- The TR characteristics of the three LIBs were remarkably distinct. The ternary lithium battery and lithium cobalt oxide battery exhibited four stages of smoke, swell, burst and stable combustion, whereas the lithium iron phosphate battery exhibited the stages of smoke, swell, burst and smoulder without a flame in the entire experiment. Furthermore, the corresponding TR critical temperatures were 260.02, 240.84 and 290.88 °C, respectively.
- With the generation of a considerable amount of smoke, CO and CO_2 gases were generated before the battery burned. The HHR and MLR increased rapidly at the steady combustion stage. The CO and CO_2 gas concentration and the LIB mass change can serve as valuable parameters for the study of TR warning index.
- The comprehensive analysis of the two experiments not only reveals that the lithium iron phosphate battery and ternary lithium battery presented higher safety and stability than the lithium cobalt oxide battery did but also showed greater significance in the potential fire or explosion hazard prevention of LIBs.

Acknowledgements The research was supported by De Montfort University through its distinguished Vice-Chancellor 2020 Programme and by the UK Science and Technology Facilities Council (STFC) through the Batteries Early Career Researcher Award.

Author contributions YX was involved in conceptualisation, resources and formal analysis. JRZ was responsible for data curation, methodology and writing—original draft. LY contributed to investigation and visualization. BL assisted with validation. YT helped with resources and writing—review and editing.

Declarations

Conflict of interest The authors declare no known competing financial interests or personal relationships that could have appeared to influence the work reported in this paper.

References

1. Netz B, Davidson OR, Bosch PR, Dave R, Meyer LA. Climate change 2007: contribution of working group III to the fourth assessment report of the intergovernmental panel on climate change. Comput Geom. 2007;18:95–123.
2. Lu LG, Han XB, Li JQ, Hua JF, Ouyang M. A review on the key issues for lithium-ion battery management in electric vehicles. J Power Sources. 2013;226:272–88.
3. Cao WJ, Lei B, Shi YJ, Dong T, Peng P, Zheng YD, et al. Ponderation over therecent safety accidents of lithium-ion battery energy storage stations in South Korea. Energy Storage Sci Technol. 2020;9:1539–47.
4. Wang Z, Yang H, Li Y, Wang G, Wang J. TR and fire behaviors of large-scale lithium ion batteries with different heating methods. J Hazard Mater. 2019;379:120730.
5. Wu TQ, Chen D, Wang QS, Sun JH. Comparison analysis on the TR of lithium-ion battery under two heating modes. J Hazard Mater. 2018;344:733–41.

6. Feng X, He XM, Ouyang M, Wang L, Lu L, Ren DS, et al. A coupled electrochemical-thermal failure model for predicting the TR behavior of lithium ion batteries. J Electrochem Soc. 2018;165:A3748–65.
7. Ren DS, Feng XN, Lu LG, Ouyang M, Zheng SQ, Li JQ, et al. An electrochemical-thermal coupled overcharge-to-thermal-runaway model for lithium ion battery. J Power Sources. 2017;364:328–40.
8. Feng XN, Lu LG, Ouyang MG, Li JQ, He XM. A 3D TR propagation model for a large format lithium ion battery module. Energy. 2016;115:194–208.
9. Noh HJ, Youn SJ, Yoon CS, Sun YK. Comparison of the structural and electrochemical properties of layered Li $[Ni_xCo_yMn_z]O_2$ (x = 1/3, 0.5, 0.6, 0.7, 0.8 and 0.85) cathode material for lithium-ion batteries. J Power Sources. 2013;233:121–30.
10. Wang QS, Ping P, Zhao XJ, Chu GQ, Sun JH, Chen CH. TR caused fire and explosion of lithium ion battery. J Power Sources. 2012;208:210–24.
11. Hossein M, Guoping D, Anaba A, Jason H. Thermal stability studies of Li-Ion cells and components. J Electrochem Soc. 1999;146(9):3224–9.
12. Liu X, Stoliarov SI, Denlinger M, Masias A, Snyder K. Comprehensive calorimetry of the thermally-induced failure of a lithium ion battery. J Power Sources. 2015;280:516–25.
13. Said AO, Lee C, Liu X, Wu ZB, Stoliarov SI. Simultaneous measurement of multiple thermal hazards associated with a failure of prismatic lithium ion battery. Proc Combust Inst. 2019;37:4173–80.
14. Balakrishnan P, Ramesh R, Kumar TP. Safety mechanisms in lithium-ion batteries. J Power Sources. 2006;155:401–3.
15. Roth EP, Doughty DH, Franklin J. DSC investigation of exothermic reactions occurring at elevated temperatures in lithium-ion anodes containing PVDF-based binders. J Power Sources. 2004;134(2):222–34.
16. Kvasha A, Gutiérrez C, Osa U, Meatza ID, Blazquez JA, Macicior H, et al. A comparative study of TR of commercial lithium ion cells. Energy. 2018;159:547–57.
17. Feng XN, Zheng SQ, Ren DS, He XM, Wang L, Liu X, et al. Key characteristics for TR of Li-ion batteries. Energy Procedia. 2019;158:4684–9.
18. Wang QS, Sun JH, Chen CH. Enhancing the thermal stability of $LiCoO_2$ electrode by 4-isopropyl phenyl diphenyl phosphate in lithium ion batteries. J Power Sources. 2006;162:1363–6.
19. Jhu CY, Wang YW, Shu CM, Chang JC, Wu HC. Thermal explosion hazards on 18650 lithium ion batteries with a VSP2 adiabatic calorimeter. J Hazard Mater. 2011;192:99–107.
20. Said M, Tohir M. Characterization of TR behaviour of cylindrical lithium-ion battery using Accelerating Rate Calorimeter and oven heating. Case Stud Therm Eng. 2021;28:101474.
21. Jin CY, Sun YD, Wang HB, Lai X, Wang SH, Chen SQ, et al. Model and experiments to investigate TR characterisation of lithium-ion batteries induced by external heating method. J Power Sources. 2021;504:230065.
22. Ping P, Wang QS, Huang PF, Li K, Sun JH, Kong DP, et al. Study of the fire behavior of high-energy lithium-ion batteries with full-scale burning test. J Power Sources. 2015;285:80–9.
23. Zhang QS, Liu TT, Wang QS. Experimental study on the influence of different heating methods on TR of lithium-ion battery. J Energy Storage. 2021;42:103063.
24. Quintiere JG. More on methods to measure the energetics of lithium ion batteries in TR. Fire Saf J. 2021;124:103382.
25. Larsson F, Mellander BE. Abuse by external heating, overcharge and short circuiting of commercial lithium-ion battery Cells. J Electrochem Soc. 2014;161:A1611–7.
26. Golubkov AW, Fuchs D, Wagner J. Thermal-runaway experiments on consumer Li-ion batteries with metal-oxide and olivin-type cathodes. RSC Adv. 2013;4:3633–42.
27. Zhu YL, Wang CJ, Gao F, Shan MX, Zhao PL, Meng QF, et al. Rupture and combustion characteristics of lithium-ion battery under overcharge. J Energy Storage. 2021;38:661–70.
28. Fu YY, Lu S, Li KY, Liu CC, Cheng XD, Zhang HP. An experimental study on burning behaviors of 18650 lithium ion batteries using a CONE. J Power Sources. 2015;273:216–22.
29. Zhong GB, Mao BB, Wang C, Jiang L, Xu KQ, Sun JH, et al. TR and fire behavior investigation of lithium ion batteries using modified CONE. J Therm Anal Calorim. 2019;135:2879–89.
30. Yang Y, Wang ZR, Guo PK, Chen SC, Bian H, Tong X, et al. Carbon oxides emissions from lithium-ion batteries under TR from measurements and predictive model. J Energy Storage. 2021;33:101863.
31. Huang PF, Yao CX, Mao BB, Wang QS, Sun JH, Bai ZH. The critical characteristics and transition process of lithium-ion battery TR. Energy. 2020;213:119082.
32. Röder P, Baba N, Wiemhöfer HD. A detailed thermal study of a $Li[Ni_{0.33}Co_{0.33}Mn_{0.33}]O_2/LiMn_2O_4$-based lithium ion cell by accelerating rate and differential scanning calorimetry. J Power Sources. 2014;248:978–87.
33. Miao Y, Hynan P, von Jouanne A, Yokochi A. Current Li-ion battery technologies in electric vehicles and opportunities for advancements. Energies. 2019;12:1074–94.
34. Zhang WJ. Structure and performance of $LiFePO_4$ cathode materials: a review. J Power Sources. 2011;196:2962–70.
35. Wang YD, Jiang JW, Dahn JR. The reactivity of delithiated $Li(Ni_{1/3}Co_{1/3}Mn_{1/3})O_2$, $Li(Ni_{0.8}Co_{0.15}Al_{0.05})O_2$ or $LiCoO_2$ with non-aqueous electrolyte. Electrochem Commun. 2007;9:2534–40.
36. Xu B, Qian D, Wang Z, Meng YS. Recent progress in cathode materials research for advanced lithium ion batteries. Mater Sci Eng R Rep. 2012;73(5–6):51–65.
37. Zhao YJ, Li J, Dahn JR. Interdiffusion of cations from metal oxide surface coatings into $LiCoO_2$ during sintering. Chem Mater. 2017;29(12):5239–48.
38. Huang ZH, Li H, Mei W, Zhao C, Sun J, Wang QS. TR behavior of lithium iron phosphate battery during penetration. Fire Technol. 2020;56(6):2405–26.
39. Huang ZH, Yu Y, Duan Q, Qin P, Sun J, Wang QS. Heating position effect on internal TR propagation in large-format lithium iron phosphate battery. Appl Energy. 2022;325:119778.
40. Chen GY, Richardson TJ. Thermal instability of Olivine-type $LiMnPO_4$ cathodes. J Power Sources. 2010;195(4):1221–4.
41. Said AO, Lee C, Stoliarov SI. Experimental investigation of cascading failure in 18650 lithium ion cell arrays: impact of cathode chemistry. J Power Sources. 2020;446:227347.
42. Bugryniec PJ, Davidson JN, Cumming DJ, Brown SF. Pursuing safer batteries: thermal abuse of $LiFePO_4$ cells. J Power Sources. 2019;414:557–68.
43. Golubkov AW, Scheikl S, Planteu R, Voitic G, Wiltsche H, Stangl C, et al. TR of commercial 18650 Li-ion batteries with LFP and NCA cathodes–impact of state of charge and overcharge. RSC Adv. 2015;5(70):57171–86.
44. Larsson F, Bertilsson S, Furlani M, Albinsson I, Mellander BE. Gas explosions and TRs during external heating abuse of commercial lithium-ion graphite-$LiCoO_2$ cells at different levels of ageing. J Power Sources. 2018;373:220–31.
45. Aurbach D, Zaban A, Ein-Eli Y, Weissman O, Chusid I, Markovsky B, et al. Recent studies on the correlation between surface chemistry, morphology, three-dimensional structures and performance of Li and Li-C intercalation anodes in several important electrolyte systems. J Power Sources. 1997;68(1):91–8.

46. Spotnitz R, Franklin J. Abuse behavior of high-power, lithium-ion cells. J power sources. 2003;113(1):81–100.